

Preparation and Characterization of $Ba_{1-x}Sr_xTiO_3$ by Sol-Gel Method

HAMED ALWAN GATEA* and IQBAL S. NAJI

Department of Physics, Science College, University of Baghdad, Baghdad, Iraq

*Corresponding author: E-mail: hamedalwan14@gmail.com

Received: 16 August 2018;

Accepted: 22 October 2018;

Published online: 30 November 2018;

AJC-19181

Barium strontium titanate (BST) with formula ($Ba_{1-x}Sr_xTiO_3$) has been synthesized by sol-gel method with different stoichiometric compositions ($x = 0.3, 0.4, 0.5, 0.6$). The raw materials which used to prepare compounds are (Ba,Sr) acetate as a source (Ba,Sr) and titanate isopropoxide source. The FE-SEM images showed that the particles size reduced from 464 to 13 nm when strontium concentration increased from 0.3 to 0.6. The X-ray diffraction studies have confirmed that $Ba_{0.7}Sr_{0.3}TiO_3$ sample have the tetragonal phase while remaining samples have a cubic phase. The intensity of the major peaks were decreased and shifted toward higher 2θ angles when Sr^{2+} ions increases.

Keywords: Ferroelectric materials, Barium strontium titanate, Curie Temperature, Perovskite structure

INTRODUCTION

Ferroelectrics technology has received extensive attention because of their ability to achieve desirable characteristics of different application due to the dependence of dielectric permittivity on the applied electric field. There are several other important ferroelectric materials. Most of the ferroelectric materials (BT, ST, BST, PZT and CT) have perovskite structure such as $PbTiO_3$, $SrBiTaO_3$, $Pb(MgNb)O_3$ and $BaTiO_3$, which are the origin of (Ba, Sr) TiO_3 [1]. A number of titanate-based ferroelectric materials have been investigated in the past for tunable device applications. These ferroelectrics are used as resonators, phase shifters, filters and capacitors in communication systems [2].

Barium strontium titanate (BST) is a ternary ceramic compound with the stoichiometric formula ($Ba_{1-x}Sr_xTiO_3$). It is a continuous solid solution containing $BaTiO_3$ and $SrTiO_3$ over the entire composition range [3]. Barium strontium titanate exhibits the high dielectric constant as that of $BaTiO_3$ and same structural stability as $SrTiO_3$ [4]. Barium strontium titanate is a material with a high degree of crystallinity, high charge storage capacity and low leakage current at Curie temperature. It has been investigated that ferroelectrics has been widely studied not only because of its variety of outstanding physical properties, but also for its practical application [5,6], such as electronic applications in multilayer and voltage-tunable capacitors, non-volatile ferroelectric memories, dynamic random access

memories (DRAM), microwave phase shifters, tunable filters, oscillators, sensors, varistors, *etc.* [7,8]. $BaSrTiO_3$ is one of the most ferroelectric materials among the complex oxide perovskite.

The physical properties have been affected by various parameters such as temperature, pressure, substitution and size due to the close relationship between ferroelectric properties and crystal structure [9]. The perovskite ABX_3 (ABO_3) structure is given in the centre (A-site, B-site, O-site). Due to the interplay of competing energies, properties can be varied significantly with a variation of concentration of Sr^{2+} ions. ABX_3 (ABO_3) has different ions that have radius B ions smaller than A ions which turn on make stabilization compound. These oxides appear different structure with different tolerance factor [10]. Also ferroelectric is mostly observed in certain temperature regions delineated by transition point (or Curie temperature, T_c) above which the crystals are no longer ferroelectrics [11]. The temperature range for which the paraelectric behaviour of barium strontium titanate can be controlled by adjusting the barium to strontium ratio [12]. The ceramic-based solid solution for barium strontium titanate with formula $Ba_{1-x}Sr_xTiO_3$ is an important candidate for a wide range of device application, special emphasis was put on compositions with ($x = 0.3$ to 0.6) [13]. At room temperature, $BaTiO_3$ has a ferroelectric or polar phase and has a ferroelectric to paraelectric transition temperature (Curie point) of $130\text{ }^\circ\text{C}$, while $SrTiO_3$ is para-

electric (non-polar) down to absolute zero. Substitution of strontium atoms in the place of barium atoms causes the Curie point to decrease linearly. It is suggested that the Curie temperature of barium strontium titanate drops to 0 °C with approximate 34 % Sr content, corresponding to a decrease of (4 °C) per molar per cent of strontium. Barium strontium titanate purely and ferroelectric and undergoes spontaneous polarization below the Curie temperature (T_C). The dielectric losses of barium strontium titanate are also high in the ferroelectric phase, above the Curie temperature, all other compositions are paraelectric and cubic [14]. Various synthesis methods for barium strontium titanate have been investigated, such as hydrothermal [15], hydrothermal-electrochemical method [16], solid state reaction [17], spray pyrolysis [18], chemical co-precipitation methods [19] and sol-gel methods [20,21]. Compared with the conventional methods, the sol-gel technique offers a homogenous distribution of elements on a molecular level, precise control of composition, high purity, lower processing temperature, lower cost and possibility for obtaining nanostructures, easy control of microstructure and crystallization rate of the final product, and the ability to coat large and complex area substrates [22,23]. In the present study, $Ba_{1-x}Sr_xTiO_3$ nanopowders were prepared with different ratio of Sr (0.3, 0.4, 0.5, and 0.6) by using sol-gel method and investigated the influence of these ratios on the microstructure and surface morphology of all powders.

EXPERIMENTAL

Synthesis of barium strontium titanate powder were mentioned in a lot of papers. The selected method for barium strontium titanate synthesis depends on some factor such as cost, low temperature and desired application. The quality of the powders affected not only synthesis route but also by starting materials used. $Ba_{1-x}Sr_xTiO_3$ nanopowders with different stoichiometric composition ($x = 0.3, 0.4, 0.5, 0.6$) were synthesized by using sol-gel method. The precursor's materials which were used in this work represent by barium acetate (99.5 % BDH Chemicals, England), strontium acetate (Aldrich 99%) and titanium (IV) isopropoxide as a source of barium, strontium and titanium respectively. Acetic acid (Aldrich 97%) was used as the solvent and 2-methoxy ethanol was used as a stabilizer for Ti(IV) isopropoxide. To obtain stoichiometric proportions appropriate weight of barium acetate and strontium acetate powder was dissolved in a suitable volume of acetic acid. The two solution separately stirred magnetically at 60 °C for 60 min, then mixed together to get (Ba,Sr) solution and refluxed at 110 °C for 2 h (till transparent solution obtained slightly tuned to yellow). 2-Methoxy ethanol (2-4 mL) was added in Ti(IV) isopropoxide at room temperature. The (Ba,Sr) solution was added slowly (dropwise) into Ti(IV) isopropoxide solution and the pH of the product solution was adjusted in the range of 3 to 5 using buffering agent. Refluxed the mixture till a thick white gel is obtained. This gel was diluted by distilled water and the solution was mixed by stirring on a hot plate (60 °C) with a magnetic stirrer. Finally, the solutions were dried at 200 °C for 2 h to separate the water completely to form amorphous powders with different compositions ($Ba_{0.7}Sr_{0.3}TiO_3$, $Ba_{0.6}Sr_{0.4}TiO_3$, $Ba_{0.5}Sr_{0.5}TiO_3$, $Ba_{0.4}Sr_{0.6}TiO_3$). The amorphous powders were calcined at 700

°C for 2 h. The powders were ground in a mortar to obtain a fine powder. The fine powders were pressed by using a hydraulic press as a pelt at pressure equals to 12000 (psi) with 1.2 cm diameter. All pellets were sintered at 1000 °C for 3 h in atmosphere. The morphological and composition properties of the sintered pellets were performed by using field emission scanning electron microscopy (FE-SEM) supplemented with energy dispersive spectroscopy model (Hitachi 4700 field emission microscope). The microstructure of all compounds were recorded at room temperature using X-ray powder diffractometer with $CuK\alpha$ ($\lambda = 1.5418 \text{ \AA}$, 30 kV, 30 mA) model (Bruker, Germany) in a wide range of $2\theta = 20^\circ-80^\circ$ at scanning rate 1 min^{-1} .

RESULTS AND DISCUSSION

Energy dispersive X-ray (EDX) analysis: In EDX spectra, the x-ray intensity is usually plotted against energy. The spectra consist of several approximately Gaussian-shaped peaks characteristic of the element present in the transmitted volume. Fig. 1 shows the EDX spectra of $Ba_{1-x}Sr_xTiO_3$ with different values of $x = 0.3, 0.4, 0.5, 0.6$ which sintered at 1000 °C for 3 h. It is clear that the elements Ba, Sr, Ti and O was detected in all spectra and there is no other elements which means that the pure barium strontium titanate phase was dominant phase, and no impurities were existed. The composition ratios (Ba/Sr) of the as-prepared powders were confirmed using the microarea EDS analysis. Stoichiometric ratios of the main metallic compounds of barium strontium titanate are shown in Table-1 as mass or atomic percentage. The result are shown in Fig. 1 are in acceptable agreement with the stoichiometric ratio for all compounds, specially $x = 0.5$.

The field emission scan electron microscopy photograph of $Ba_{1-x}Sr_xTiO_3$ gel for $x = 0.3$ and 0.4 are shown in Fig. 2a-b, respectively. It can be observed that barium strontium titanate particles in the nanoscale, where the particles diameter in the range 12-18 nm for $x = 0.3$ and 10-15 nm for $x = 0.4$. The powder samples calcined for 2 h at 700 °C for $x = 0.3$ and 0.4 are illustrated in Fig. 2c-d, respectively. The particles are spherical in nature with size in the range of 26-42 nm and 22-37 nm for $x = 0.3$ and 0.4 , respectively.

Fig. 3 shows the surface morphologies of the barium strontium titanate powders sintered at 1000 °C for 3 h for different x values. The particles are a mixture of spherical and nearly cubic in nature and less agglomerated specially for $x = 0.3$ and 0.4 (Fig. 3a-b). When Sr^{2+} content increases to $x = 0.5$ and 0.6 , the particle tend to be spherical shape and small grains merged with each other to become larger ones. The synthesis parameters such as initial concentration and reaction time (stirrer and reflux time) have a great influence on the size of nanostructure of barium strontium titanate. By controlling on these parameters the particles size change to be (464, 79.80, 63.09, 46, 13 nm) for $x = 0.3, 0.4, 0.5$ and 0.6 , respectively. It is clear that the particles size of barium strontium titanate decreases with an increment of Sr^{2+} ions due to the small radius for strontium ion. This result agreed with the results of Azim *et. al.* [3] and Gao *et al.* [24].

XRD analysis: The structure of $Ba_{1-x}Sr_xTiO_3$ powders with different x values which had been produced by sol-gel method is shown in Fig. 4 which revealed that all the samples are polycrystalline in nature.

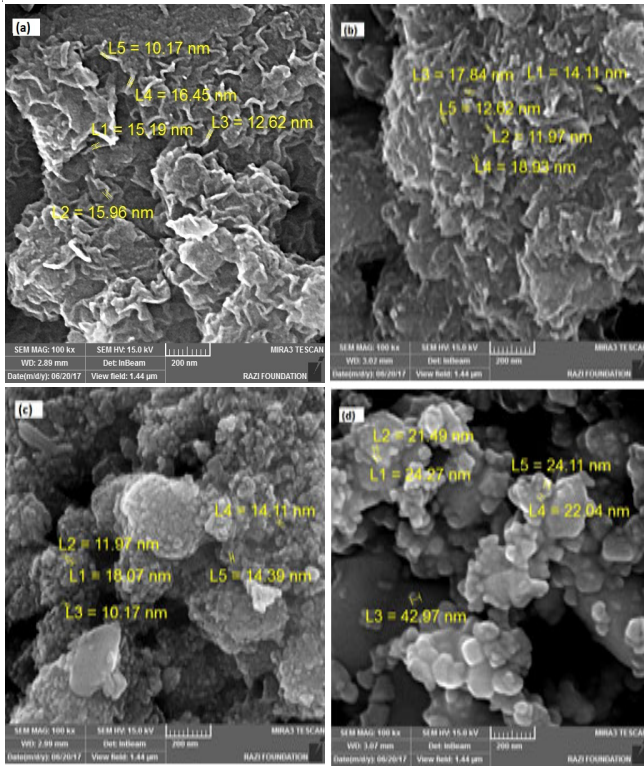


Fig. 2. Field emission scanning electron microscopy (FE-SEM) images for $Ba_{1-x}Sr_xTiO_3$ (a) $x = 0.3$ gel, (b) $x = 0.4$ gel, (c) $x = 0.3$ powder and (d) $x = 0.4$ powder calcined at $700^\circ C$

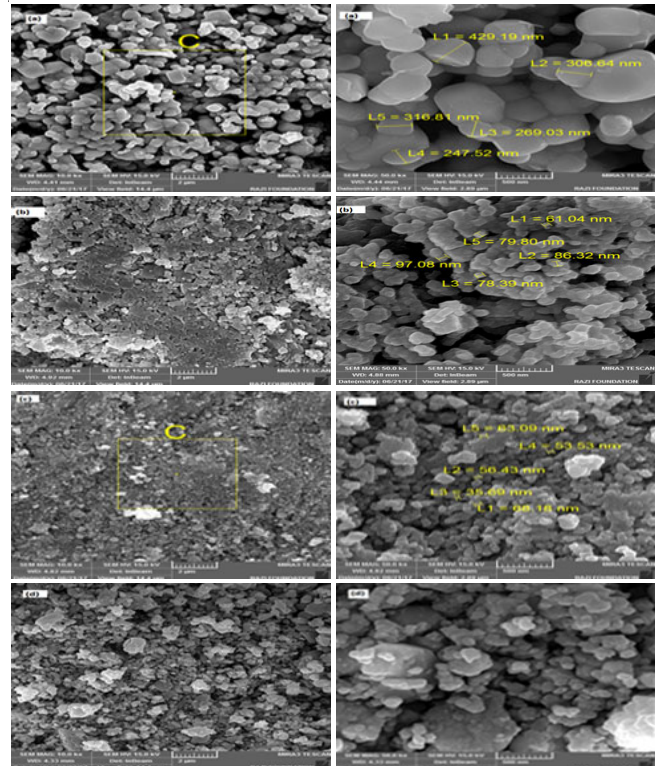


Fig. 3. Field emission scanning electron microscopy (FE-SEM) images for $Ba_{1-x}Sr_xTiO_3$ powders sintered at $1000^\circ C$ (a) $x = 0.3$, (b) $x = 0.4$, (c) $x = 0.5$ and (d) $x = 0.6$

TABLE-2

STRUCTURAL PARAMETERS *viz.* 2θ VALUES, INTER-PLANAR SPACING, MILLER INDICES AND PHASE OF $Ba_{1-x}Sr_xTiO_3$ POWDERS

x	2θ ($^\circ$)	d_{hkl} Exp. (\AA)	d_{hkl} Std. (\AA)	hkl	Phase	Card No.
0.3	22.3357	3.9771	3.977	(100)	Tetragonal	00-044-0039
	31.7474	2.8122	2.8162	(101)	Tetragonal	00-044-0039
	39.1636	2.2961	2.2983	(111)	Tetragonal	00-044-0039
	45.5616	1.9885	1.9885	(200)	Tetragonal	00-044-0039
	51.3214	1.7786	1.7795	(201)	Tetragonal	00-044-0039
	56.6061	1.6215	1.6246	(211)	Tetragonal	00-044-0039
	66.3277	1.4060	1.4080	(202)	Tetragonal	00-044-0039
70.9422	1.2576	1.2610	(212)	Tetragonal	00-044-0039	
0.4	22.3984	3.9600	3.9660	(100)	Cubic	00-034-0411
	31.8658	2.8036	2.8060	(110)	Cubic	00-034-0411
	39.3113	2.2891	2.2900	(111)	Cubic	00-034-0411
	45.7322	1.9825	1.9823	(200)	Cubic	00-034-0411
	51.4850	1.7732	1.7735	(210)	Cubic	00-034-0411
	56.8005	1.6195	1.6190	(211)	Cubic	00-034-0411
	66.6377	1.4018	1.4023	(220)	Cubic	00-034-0411
71.3196	1.2537	1.2530	(221)	Cubic	00-034-0411	
0.5	22.4934	3.9470	3.9494	(100)	Cubic	00-039-1395
	32.0312	2.7909	2.7918	(110)	Cubic	00-039-1395
	39.4971	2.2788	2.2796	(111)	Cubic	00-039-1395
	45.9429	1.9735	1.9737	(200)	Cubic	00-039-1395
	51.7535	1.7651	1.7649	(210)	Cubic	00-039-1395
	57.1126	1.6113	1.6113	(211)	Cubic	00-039-1395
	67.0089	1.3954	1.3954	(220)	Cubic	00-039-1395
71.6718	1.2481	1.2480	(221)	Cubic	00-039-1395	
0.6	22.5516	3.9390	3.9394	(100)	Cubic	01-078-2723
	32.1057	2.7852	2.7855	(110)	Cubic	01-078-2723
	39.5920	2.2741	2.2744	(111)	Cubic	01-078-2723
	45.0415	1.9695	1.9697	(200)	Cubic	01-078-2723
	51.8538	1.7615	1.7617	(210)	Cubic	01-078-2723
	57.2344	1.6080	1.6080	(211)	Cubic	01-078-2723
	67.1500	1.3926	1.3927	(220)	Cubic	01-078-2723
71.8320	1.2456	1.2457	(221)	Cubic	01-078-2723	

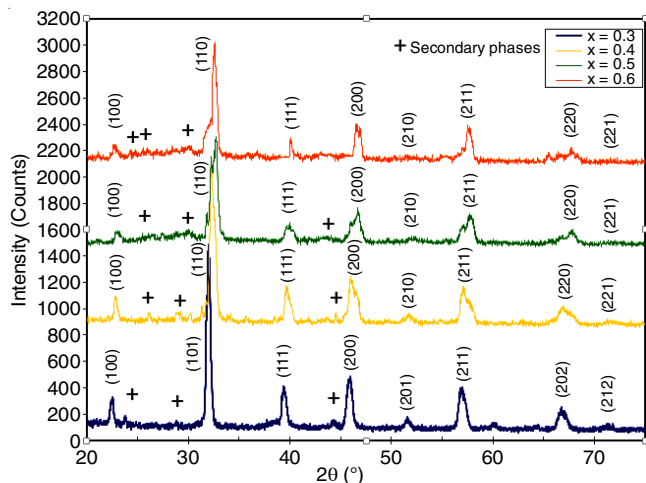


Fig. 4. XRD patterns of $Ba_{1-x}Sr_xTiO_3$ powders with various ratio of x

agreement with the cubic barium strontium titanate phase (JCPDS card no.00-039-1395).

The XRD pattern of $Ba_{0.4}Sr_{0.6}TiO_3$ shows the presence of a number of peaks along the (100), (110), (111), (200), (210), (211), (220) and (221). These peaks are in good agreement with the cubic BST phase (JCPDS card no. 01-078-2723). From XRD analysis, it can be estimated that the tetragonal phase of $x = 0.3$ transform to cubic phase with increasing Sr ratio to 0.4, 0.5 and 0.6.

There are also two weak diffraction peaks as a secondary phase besides the peaks of barium strontium titanate phase, which appeared at ($2\theta = 24.21^\circ, 26.80^\circ$) and (28.80°) belong to intermediate oxycarbonates such as $Ba_2Ti_2O_5CO_3$ and $(Ba,Sr)Ti_2O_5CO_3$ [2,3,25,26]. The most probable crystalline impurity are Sr_2TiO_4 , $SrTiO_{10}$, $Sr_3Ti_2O_7$ almost appear at 44.6° [2,25]. The major peaks shifted toward higher 2θ angles when Sr^{2+} ions increases. This happened due to the decrease interatomic spacing of barium strontium titanate which affected by the radius of Sr^{2+} ion (1.13 \AA) which is smaller than Ba^{2+} ions (1.35 \AA).

Conclusion

The barium strontium titanate powders with different stoichiometric composition ($Ba_{1-x}Sr_xTiO_3$) has been successfully synthesized by sol-gel method. The synthesis of ceramics materials from barium acetate, strontium acetate and titanate isopropoxide with a solvent such as acetic acid and 2-methoxy ethanol. EDX spectra of as-prepared $Ba_{1-x}Sr_xTiO_3$ nanoparticles contains Ba, Sr, Ti and O species and the all experimental ratios of Ba/Sr are closely to exact values. FE-SEM investigations showed that the nanoparticles obtained at 1000°C more larger in size than obtained at 700°C and the particle size reduced with increasing Sr ratio. The good crystalline ceramic samples exhibit the regular of different space group ($P4mm, Pm3m, Pm3m, P3mm$) for $x = 0.3, 0.4, 0.5$ and 0.6 respectively, after sintering at 1000°C for 3 h. The increasing strontium ratio leading to change the phase from tetragonal to cubic when x value change from 0.3 to 0.4, 0.5, 0.6 and the d -space values decreased with increased strontium ions.

ACKNOWLEDGEMENTS

The authors the financial support from University of Baghdad, Baghdad, Iraq.

CONFLICT OF INTEREST

The authors declare that there is no conflict of interests regarding the publication of this article.

REFERENCES

1. F. Dogan, H. Lin, M. Guilloux-Viry and O. Peña, *Sci. Technol. Adv. Mater.*, **16**, 020301 (2015); <https://doi.org/10.1088/1468-6996/16/2/020301>.
2. V. Somani and S.J. Kalita, *J. Electroceram.*, **18**, 57 (2007); <https://doi.org/10.1007/s10832-007-9008-7>.
3. M.E. Azim Araghi, N. Shaban and M. Bahar, *Mater. Sci. Poland*, **34**, 63 (2016); <https://doi.org/10.1515/msp-2016-0020>.
4. P.K. Sharma, G.L. Messing and D.K. Agrawal, *Thin Solid Films*, **491**, 204 (2005); <https://doi.org/10.1016/j.tsf.2004.08.171>.
5. A. Selmi, O. Khaldi, M. Mascot, F. Jomni and J.C. Carru, *J. Mater. Sci. Mater. Electron.*, **27**, 11299 (2016); <https://doi.org/10.1007/s10854-016-5253-3>.
6. F.M. Pontes, E. Leite, D. Pontes, E. Longo, S. Mergulhão, E.M.S. Santos, P.S. Pizani, F. Lanciotti Jr., T.M. Boschi and J.A. Varela, *J. Appl. Phys.*, **91**, 5972 (2002); <https://doi.org/10.1063/1.1466526>.
7. J. Zhao, X. Wang, R. Chen and L. Li, *Mater. Lett.*, **59**, 2329 (2005); <https://doi.org/10.1016/j.matlet.2005.02.075>.
8. S. Kribalis, P.E. Tsakiridis, C. Dedeloudis and E. Hristoforou, *J. Optoelectron. Adv. Mater.*, **8**, 1475 (2006).
9. P.M. Kshirsagar, P.P. Khirade, D.N. Bhojar, S.J. Shukla and K.M. Jadhav, *Int. J. Innov. Sci. Eng. Technol.*, **4**, 5 (2017).
10. R.S. Roth, *J. Res. Natl. Bur. Stand.*, **58**, 75 (1957); <https://doi.org/10.6028/jres.058.010>.
11. Y. Xu, *Ferroelectric Materials and their Application*, University of California, Los Angeles, USA, Published by North-Holland, pp. 1–36 (1991).
12. A.B. Catalan, J.V. Mantese, A.L. Micheli and N.W. Schubring, *J. Appl. Phys.*, **76**, 2541 (1994); <https://doi.org/10.1063/1.357568>.
13. A. Ioachim, M.I. Toacsan, M.G. Banciu, L. Nedelcu, A. Dutu, S. Antohe, C. Berbecaru, L. Georgescu, G. Stoica and H.V. Alexandru, *Thin Solid Films*, **515**, 6289 (2007); <https://doi.org/10.1016/j.tsf.2006.11.097>.
14. S.F. Mohiuddin, Ph.D. Thesis, Northern Illinois University, Illinois:USA (2011).
15. D. Gao, D. Xiao, J. Bi, P. Yu, G. Yu, W. Zhang and J. Zhu, *Mater. Trans.*, **44**, 1320 (2003).
16. S. Agarwal and G.L. Sharma, *Sens. Actuators B Chem.*, **85**, 205 (2002); [https://doi.org/10.1016/S0925-4005\(02\)00109-0](https://doi.org/10.1016/S0925-4005(02)00109-0).
17. Y.J. Wu, Y.H. Huang, N. Wang, J. Li, M.S. Fu and X.M. Chen, *J. Eur. Ceram. Soc.*, **37**, 2099 (2017); <https://doi.org/10.1016/j.jeurceramsoc.2016.12.052>.
18. N. Golego, S.A. Studenikin and M. Cocivera, *Chem. Mater.*, **10**, 2000 (2000); <https://doi.org/10.1021/cm980153+>.
19. F. Schrey, *J. Am. Ceram. Soc.*, **48**, 401 (1965); <https://doi.org/10.1111/j.1151-2916.1965.tb14776.x>.
20. Y. Seo and S. Park, *J. Korean Phys. Soc.*, **45**, 1 (2004).
21. T. Zhang and H. Ni, *Sens. Actuators A Phys.*, **100**, 252 (2002); [https://doi.org/10.1016/S0924-4247\(02\)00139-5](https://doi.org/10.1016/S0924-4247(02)00139-5).
22. A. Khalfallaoui, G. Vélou, L. Burgnies and J.E. Carru, *IEEE Trans. Ultrason., Ferroelect. Freq. Contr.*, **57**, 1029 (2010); <https://doi.org/10.1109/TUFFC.2010.1514>.
23. J. Zhai and H. Chen, *J. Korean Ceram. Soc.*, **40**, 380 (2003); <https://doi.org/10.4191/kcers.2003.40.4.380>.
24. Y. Gao, V.V. Shvartsman, D. Gautam, M. Winterer and D.C. Lupascu, *J. Am. Ceram. Soc.*, **97**, 2139 (2014); <https://doi.org/10.1111/jace.12933>.
25. U. Adem, Ph.D. Thesis, Middle East Technical University: Ankara, Turkey (2003).
26. M.C. Gust, L.A. Momoda, N.D. Evans and M.L. Mecartney, *J. Am. Ceram. Soc.*, **84**, 1087 (2001); <https://doi.org/10.1111/j.1151-2916.2001.tb00794.x>.